# A controlling role for the air–sea interface in the chemical processing of reactive nitrogen in the coastal marine boundary layer

Michelle J. Kim[a], Delphine K. Farmer[b], and Timothy H. Bertram[c,1]

[a]Scripps Institution of Oceanography and [c]Department of Chemistry and Biochemistry, University of California, San Diego, La Jolla, CA 92093; and [b]Department of Chemistry, Colorado State University, Fort Collins, CO 80523

Edited by A. R. Ravishankara, Colorado State University, Fort Collins, CO, and approved February 10, 2014 (received for review October 3, 2013)

**The lifetime of reactive nitrogen and the production rate of reactive halogens in the marine boundary layer are strongly impacted by reactions occurring at aqueous interfaces. Despite the potential importance of the air–sea interface in serving as a reactive surface, few direct field observations are available to assess its impact on reactive nitrogen deposition and halogen activation. Here, we present direct measurements of the vertical fluxes of the reactant–product pair $N_2O_5$ and $ClNO_2$ to assess the role of the ocean surface in the exchange of reactive nitrogen and halogens. We measure nocturnal $N_2O_5$ exchange velocities ($V_{ex} = -1.66 \pm 0.60$ cm $s^{-1}$) that are limited by atmospheric transport of $N_2O_5$ to the air–sea interface. Surprisingly, vertical fluxes of $ClNO_2$, the product of $N_2O_5$ reactive uptake to concentrated chloride containing surfaces, display net deposition, suggesting that elevated $ClNO_2$ mixing ratios found in the marine boundary layer are sustained primarily by $N_2O_5$ reactions with aerosol particles. Comparison of measured deposition rates and in situ observations of $N_2O_5$ reactive uptake to aerosol particles indicates that $N_2O_5$ deposition to the ocean surface accounts for between 26% and 42% of the total loss rate. The combination of large $V_{ex, N2O5}$ and net deposition of $ClNO_2$ acts to limit $NO_x$ recycling rates and the production of Cl atoms by shortening the nocturnal lifetime of $N_2O_5$. These results indicate that air–sea exchange processes account for as much as 15% of nocturnal $NO_x$ removal in polluted coastal regions and can serve to reduce $ClNO_2$ concentrations at sunrise by over 20%.**

heterogeneous chemistry | halogen chemistry | atmospheric chemistry

The production rate of tropospheric ozone ($O_3$), a criteria air pollutant, depends critically on the concentrations of nitrogen oxides ($NO_x \equiv NO + NO_2$), volatile organic compounds (VOCs), trace oxidants (e.g., OH, $NO_3$, and Cl), and the wavelength-dependent actinic flux. Accurate model representation of $O_3$ mixing ratios and the sensitivity of $O_3$ to changes in $NO_x$ and VOC emissions rely heavily on a complete description of the factors that control $NO_x$ lifetimes and, in turn, the concentrations of atmospheric oxidants. Modeling studies, constrained by laboratory and field observations, suggest that nocturnal processes involving the nitrate radical ($NO_3$) and $N_2O_5$, both products of $NO_x$ oxidation, can account for as much as 50% of the $NO_x$ removal (1). Incorporation of the heterogeneous reaction of $N_2O_5$ on chloride containing aerosol particles (2, 3) serves as both an efficient $NO_x$ recycling and halogen activation mechanism via the production of photolabile nitryl chloride ($ClNO_2$) in both coastal (4) and continental air masses (5).

To date, study of the impact of nocturnal processes on the lifetime of $NO_x$ and the production of reactive halogen species in the marine boundary layer has concentrated on gas-phase reactions and heterogeneous and multiphase processes occurring on/within aerosol particles, with little attention paid to reactions occurring at the air–sea interface (6, 7). With nearly half of Earth's population living within 200 km of a saltwater coastline, a significant fraction of $NO_x$ emissions are found near coastal waters (4, 8). As such, the chemical evolution of polluted air masses stemming from coastal megacities occurs to a large extent over the ocean (e.g., Beijing plume). If air–sea exchange of reactive nitrogen compounds is rapid and the reaction kinetics at the air–ocean and air–particle surface are comparable, we expect air–sea exchange processes to play an important role in setting the lifetime of compounds such as $N_2O_5$ in coastal environments. Specifically, dry deposition of $N_2O_5$ to the ocean surface could serve to help close the existing gap between models and measurements of $N_2O_5$ mixing ratios in the polluted marine boundary layer (9). In what follows, we describe direct measurements of the vertical flux of $N_2O_5$ and $ClNO_2$ obtained via eddy covariance at a polluted coastal site to provide observation-based constraints on the role of the air–sea interface in setting the lifetime of reactive nitrogen and the production rate of reactive halogens in the marine boundary layer.

The vertical flux of trace gases across the air–sea interface is a complex function of both atmospheric and oceanic processes, where gas exchange is controlled by molecular diffusion in the interfacial regions surrounding the air–water interface (10) and the solubility and chemical reactivity of the gas in the molecular sublayer. The flux ($F$) of trace gas across the interface is described by Eq. **E1**, as a function of both the gas-phase ($C_g$) and liquid phase ($C_l$) concentrations and the dimensionless gas over liquid Henry's law constant ($K_H$),

$$F = -K_t\left(C_g - K_H C_l\right), \qquad \textbf{[E1]}$$

where $K_t$, the total transfer velocity for the gas (cm $s^{-1}$), encompasses all of the chemical and physical processes that govern

## Significance

Reactions occurring at the air–sea interface have the potential to alter the chemical composition of the atmosphere. However, our knowledge of the extent to which these reactions impact the concentration of oxidants and their precursors is derived from laboratory measurements using systems that mimic the chemical, biological, and physical complexity of the surface ocean. Here, we present direct measurements of the vertical fluxes of a reactant–product pair using eddy covariance coupled with chemical ionization time-of-flight mass spectrometry to directly assess the role of the ocean surface in the exchange of reactive nitrogen and halogens. Our observations suggest that the ocean surface plays a critical role in controlling the lifetime of $N_2O_5$, a primary nocturnal reservoir for tropospheric reactive nitrogen.

Author contributions: T.H.B. designed research; M.J.K. performed research; M.J.K., D.K.F., and T.H.B. analyzed data; and M.J.K., D.K.F., and T.H.B. wrote the paper.

The authors declare no conflict of interest.

This article is a PNAS Direct Submission.

[1]To whom correspondence should be addressed. E-mail: thbertram@ucsd.edu.

This article contains supporting information online at www.pnas.org/lookup/suppl/doi:10.1073/pnas.1318694111/-/DCSupplemental.

air–sea gas exchange (11). As such, accurate, molecule-specific parameterization of $K_t$ is critical for assessing the role of the ocean as a net source or sink for both greenhouse gases and criteria air pollutants, and the trace gases that control their abundances in the atmosphere.

With respect to $N_2O_5$ air–sea exchange, we expect the reaction mechanism to closely follow that described for reactions occurring at the air–particle interface, particularly that of sea spray aerosol. Generally, the reactive uptake of $N_2O_5$ to aqueous interfaces in the troposphere has been proposed to follow the concerted reaction mechanism (12, 13):

$$N_2O_{5(gas)} \overset{k_1,k_{-1}}{\longleftrightarrow} N_2O_{5(aq)}, \qquad \textbf{[R1]}$$

$$N_2O_{5(aq)} + H_2O_{liq} \xrightarrow{k_2} H_2ONO^+_{2(aq)} + NO^-_{3(aq)}, \qquad \textbf{[R2a]}$$

$$H_2ONO^+_{2(aq)} + NO^-_{3(aq)} \xrightarrow{k_{-2}} N_2O_{5(aq)} + H_2O_{liq}, \qquad \textbf{[R2b]}$$

$$H_2ONO^+_{2(aq)} + H_2O_{liq} \xrightarrow{k_3} H_3O^+_{(aq)} + HNO_{3(aq)}, \qquad \textbf{[R3]}$$

$$H_2ONO^+_{2(aq)} + X^- \xrightarrow{k_4} XNO_2 + H_2O_{liq}. \qquad \textbf{[R4]}$$

This mechanism is consistent with laboratory evidence that the reactive uptake of $N_2O_5$ to aqueous interfaces is dependent on: (*i*) liquid water content (13), (*ii*) nitrate ($NO_3^-$) and chloride ($Cl^-$) concentrations (13–15), and (*iii*) the presence of organic surfactants and/or films (16–19). The $ClNO_2$ product yield, $\Phi$ ($ClNO_2$), following $N_2O_5$ hydrolysis has been shown to be a strong function of chloride concentration, where $\Phi$ ($ClNO_2$) is 0.8 for $[Cl^-] = 0.5$ M, increasing to 1.0 for $[Cl^-] > 1.0$ M (2, 13, 20).

Extension of laboratory determined reaction rates (21) and equilibrium constants (2, 22) to the air–sea interface would suggest that $N_2O_5$ deposition to the ocean should be rapid (e.g., $K_H = 1.9 \times 10^{-2}$, $k_2 = 5 \times 10^6$ s$^{-1}$) and that $\Phi$ $(ClNO_2)_{ocean}$ would be >0.8, based on an oceanic $[Cl^-]$ of 0.55 M. However, the a priori estimate for the magnitude and direction of the air–sea flux for $ClNO_2$ ($K_H = 1.66$) is less clear (2). Although laboratory results suggest that $ClNO_2$ should be made at high yield at the ocean surface, it is not clear if water-side transport and subsequent chemical reactions may suppress $ClNO_2$ release back to the atmosphere. Alternatively, reaction of the nitronium ion ($NO_2^+$) in the organic-rich sea surface microlayer (23) may also serve to reduce $\Phi$ $(ClNO_2)_{ocean}$, a reaction that may also proceed in organic-rich aqueous aerosol.

## Results and Discussion

**Eddy Covariance Measurements of $N_2O_5$ and $ClNO_2$ Air–Sea Exchange.** Concentration and vertical flux measurements of $N_2O_5$ and $ClNO_2$ were made at 13 m above mean lower low water (13 m above mean low water) from the end of the 330-m Scripps Institution of Oceanography (SIO) pier during January and February 2013. Briefly, $N_2O_5$ and $ClNO_2$ mixing ratios were measured using chemical ionization time-of-flight mass spectrometry (24), using $I^-$ reagent ion chemistry (25). Spectra were saved at 10 Hz, coincident in time with measurements of 3D winds acquired with a colocated ultrasonic anemometer sampling at 20 Hz. Details on instrument calibration, inlet performance, and flux measurements can be found in *Materials and Methods* and *SI Text*.

Here, we discuss a subset of these measurements obtained on February 20, 2013 where the true wind direction ranged between 205° and 295°, resulting in a purely ocean fetch with pollution from Los Angeles entrained into the sampled air mass. Ten-meter wind speeds ($u_{10}$) ranged between 6.5 and 11.1 m s$^{-1}$ with a mean and SD of 9.07 ± 1.29 m s$^{-1}$. The diel profile in $N_2O_5$ and $ClNO_2$ mixing ratios is shown in Fig. 1 *A* and *B*, where $N_2O_5$ and $ClNO_2$ mixing ratios track one another for much of the night, peaking at midnight. As expected, $N_2O_5$ mixing ratios drop sharply to zero at sunrise due to rapid photolysis of the nitrate radical ($NO_3$), which is in thermal equilibrium with $N_2O_5$, whereas $ClNO_2$ decays to zero with a time constant ($\tau = 2.71$ h) consistent with its photolysis lifetime (26). The magnitude of the $N_2O_5$ and $ClNO_2$ mixing ratios are comparable with those found in previous studies in coastal California (27).

$N_2O_5$ flux measurements are shown in Fig. 2*A*. As expected, $N_2O_5$ displays a net downward flux, into the ocean. The magnitude of the flux tracks ambient $N_2O_5$ mixing ratios, yielding a nocturnally averaged exchange velocity ($V_{ex}$, or flux divided by concentration) of −1.66 ± 0.60 (1σ) cm s$^{-1}$. We note that a negative $V_{ex}$ indicates a downward flux from the atmosphere to the ocean. $V_{ex,N2O5}$ can be interpreted within the resistance framework developed for $O_3$ dry deposition, where $V_{ex}$ depends on the aerodynamic resistance, quasi-laminar boundary layer resistance, and the surface resistance that includes chemical reactions at the interface (28). To this end, we calculate the total transfer velocity ($K_t$) for $N_2O_5$ (Eq. **E2**) for comparison with the observed exchange rate,

$$K_t = \left[\frac{1}{k_a} + \frac{K_H}{k_w}\right]^{-1}, \qquad \textbf{[E2]}$$

where $k_a$ is the air-side transfer velocity, $k_w$ is the water-side transfer velocity, and $K_H$ is the dimensionless gas over liquid Henry's law constant. Over the past two decades, a series of parameterizations (ref. 11 and references therein) have been developed that permit calculation of both $k_a$ and $k_w$ as a function of both the molecular properties of the gas (e.g., diffusivity, reactivity, solubility) and physical forcing data (e.g., wind speed). In the case of $N_2O_5$, the hydrolysis rate ($k_2$) is sufficiently fast (>$1 \times 10^6$ s$^{-1}$) that we expect $N_2O_5$ deposition to be limited only by the air-side transfer rate ($k_a$), despite its moderate solubility ($K_H = 1.9 \times 10^{-2}$). As such, we calculate $k_a$ (Eq. **E3**) following the numerical approach of Johnson (29) where the still air diffusive flux of Mackay and Yeun (30) has been added to the representation of $k_a$ found in the NOAA COARE model (31), with a numerical representation of the wind speed dependent drag coefficient ($C_D$).

$$k_a = 1 \times 10^{-3} + \frac{u^*}{13.3S_c^{\frac{1}{2}} + C_D^{-\frac{1}{2}} - 5 + \frac{\ln(S_c)}{(2\kappa)}} \qquad \textbf{[E3]}$$

Here, $u^*$ is the friction velocity, $S_c$ is the Schmidt number for $N_2O_5$, and κ is the von Karman constant (taken as 0.4). For

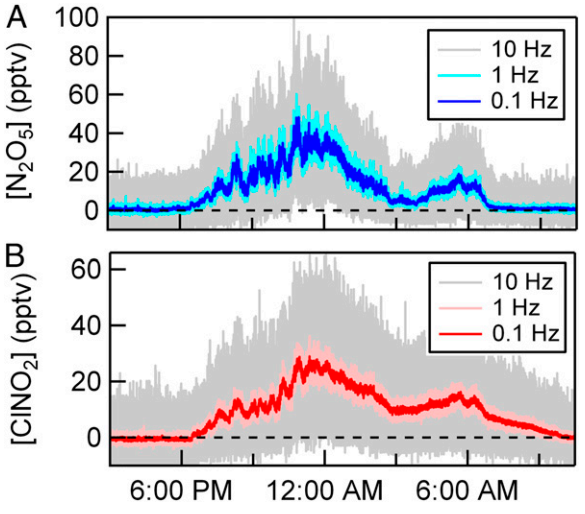


**Fig. 1.** (*A*) $N_2O_5$ and (*B*) $ClNO_2$ mixing ratios as measured from the SIO pier in La Jolla, CA, on February 20, 2013 at 0.1, 1, and 10 Hz time resolution.

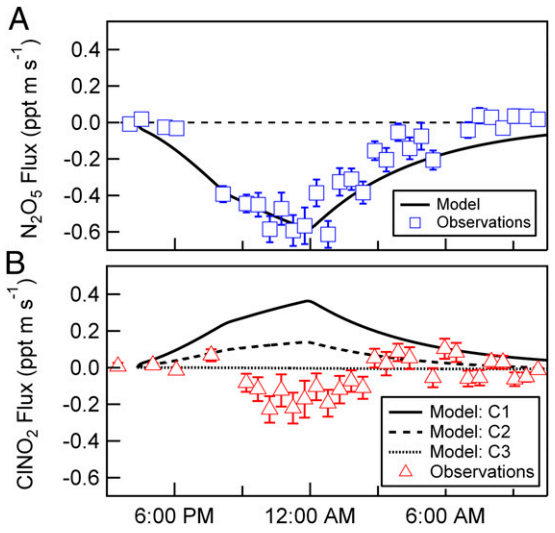


**Fig. 2.** Measured vertical fluxes of $N_2O_5$ and $ClNO_2$. Errors are determined for each 30-min flux segment as the covariance between vertical wind speed and concentration at lag times significantly longer than the delay (or lag) time. Calculated $ClNO_2$ vertical fluxes (lines in *B*), as determined from the coupled time-dependent ocean–atmosphere model, constrained by the measured $N_2O_5$ vertical fluxes (*A*). Three different model scenarios are shown and described in detail in *SI Text*: C1 (a priori), model inputs taken as suggested in the literature [e.g., $K_H$ ($ClNO_2$) = 1.66, $\Phi$ $(ClNO_2)_{ocean}$ = 0.8, $k_r = 5 \times 10^6$ s$^{-1}$, and $\delta = 1.5 \times 10^{-6}$ cm]; C2, model inputs taken as 90% confidence limits of those suggested in the literature [e.g., $K_H$ ($ClNO_2$) = 0.32, $\Phi$ $(ClNO_2)_{ocean}$ = 0.5, $k_r = 2 \times 10^5$ s$^{-1}$, and $\delta = 7.1 \times 10^{-6}$ cm]; and C3, same as C2, with $\Phi$ $(ClNO_2)_{ocean}$ = 0.

comparison, if we neglect fast hydrolysis, $N_2O_5$ deposition is controlled by the surface resistance due to its moderate solubility and slow diffusion rate in water ($D_l = 1.9 \times 10^{-5}$ cm$^2$ s$^{-1}$) (32). Calculations of the total transfer velocity of $N_2O_5$ as a function of wind speed are shown in Fig. 3, with (solid black line) and without (dashed black line) surface hydrolysis. In the latter case, we calculate $k_w$, again following the numerical approach of Johnson (29). Also included in Fig. 3 are the wind speed-dependent parameterizations for $k_a(N_2O_5)$ of Liss (33) and Mackay and Yeun (30) both derived from wind tunnel studies and that of Duce et al. (34), which is calculated from micrometeorological theory. The nocturnally averaged measured $N_2O_5$ exchange velocity is shown with a blue square in Fig. 3. As shown, the observed exchange rate is on average a factor of 2.17 larger than that calculated using Eq. **E3**; however, it is in agreement with the parameterizations of Liss (10) and Mackay and Yeun (30), to within the uncertainty and variability of the measurements. Longer-term observations of $F_{N2O5}$, designed to capture wide variability in wind speed, will provide unique observation-based constraints on $k_a$, while permitting the opportunity to assess the impact of entrainment of $N_2O_5$ and $ClNO_2$ from the free troposphere and vertical gradients in temperature and aerosol surface area on the retrieved fluxes.

Our a priori supposition for the direction of the $ClNO_2$ flux, based on laboratory-determined reaction rates and equilibrium constants, is assumed to be out of the ocean, where hydrolyzed $N_2O_5$ produces $NO_2^+$ ions that rapidly react with $Cl^-$, forming $ClNO_2$ in high yield at the ocean surface. Given the $N_2O_5$ deposition rate measured above, combined with the moderate solubility of $ClNO_2$, one would expect the magnitude of the flux to be nearly equal, yet opposite in direction, to $N_2O_5$. Surprisingly, vertical fluxes of $ClNO_2$ show net deposition, with the exception of the time period between 0300 and 0600, where the $ClNO_2$ flux indicates net emission from the sea surface (Fig. 2*B*).

**Modeling Sea Surface Chemistry of Deposited $N_2O_5$.** To further our understanding of $N_2O_5$ reactions at the ocean interface, we construct a coupled atmosphere–surface ocean time-dependent box model following the framework outlined in Carpenter et al. (35). The model is constrained by the measured $N_2O_5$ vertical flux reported above and $N_2O_5$ and $ClNO_2$ reaction rates, product branching ratios, and diffusion constants as previously determined in the literature for reactions occurring at the air–particle interface. As in Carpenter et al. (35), we define a surface aqueous layer ($\delta$) with a depth equal to the reacto-diffusive length (Eq. **E4**) for the $N_2O_5$ reaction mechanism (Reactions **R1**–**R4**)

$$\delta = \sqrt{\frac{D_l}{k_r}}, \qquad \textbf{[E4]}$$

where $D_l$ is the $N_2O_5$ liquid-phase diffusion constant ($D_l = 1.9 \times 10^{-5}$ cm$^2$ s$^{-1}$) (32), and $k_r$ is the total reactivity of $N_2O_5$ in seawater ($k_r$), taken as the $N_2O_5$ hydrolysis rate ($k_2$) (21) as the lifetime of the nitronium ion ($NO_2^+$) product is estimated to be less than $10^{-9}$ s, making the hydrolysis the rate limiting step in the mechanism (2). We expect the reaction to occur in a thin film ($\delta$ < 100 nm), well within the molecular sublayer (*ca.* $10^{-3}$ m) where transport is driven by molecular diffusion (28). As a result, rapid volatilization of reaction products of relatively high solubility may occur following the supersaturation of dissolved gas in the thin film. For simplicity, gas transfer velocities ($K_t$) and the associated vertical flux for $ClNO_2$ are calculated in the model using $k_a$ (Eq. **E1**) and $k_w$ (Eq. **E2**) parameterizations as described in Johnson (29). As in Carpenter et al. (35), mixing from the bulk, where [$ClNO_2$] is taken to be zero, to the interfacial region is determined by the wind speed dependent expression for the transfer velocity.

To explore the apparent downward measured flux of $ClNO_2$, we drive the coupled atmosphere–ocean model using three plausible sets of input values in the treatment of $K_t$. In model case 1 (C1), our a priori conditions were based on existing laboratory-based measurements, where model input parameters were taken as suggested in the literature: $K_H$ ($ClNO_2$) = 1.66, $\Phi$ $(ClNO_2)_{ocean}$ = 0.8, $k_r = 5 \times 10^6$ s$^{-1}$, and $\delta = 1.5 \times 10^{-6}$ cm. As

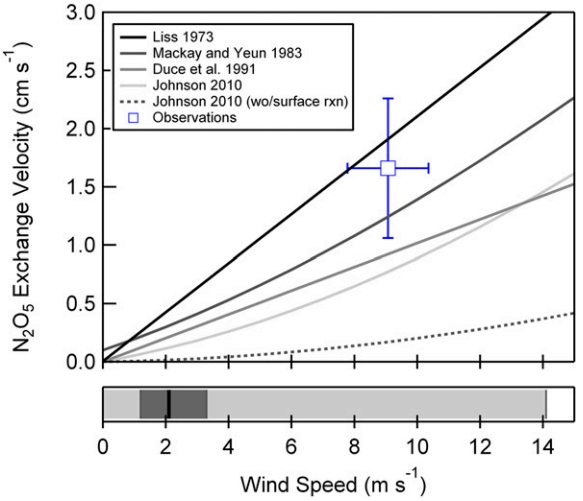


**Fig. 3.** (*Upper*) Average $N_2O_5$ exchange velocity ($V_{ex}$, cm s$^{-1}$) as a function of 10-m wind speed (m s$^{-1}$). Modeled exchange velocities, determined via Eq. **E3** [Johnson (29)] are shown using the dimensionless gas over liquid Henry's Law Constant, $K_H$ ($N_2O_5$) = $1.9 \times 10^{-2}$ with and without incorporation of $N_2O_5$ hydrolysis ($k_r = 5 \times 10^6$ s$^{-1}$). Parameterizations of Liss (33), Mackay and Yeun (30), and Duce (34) are also shown for comparison. (*Lower*) The 2012 annual median (black line), interquartile range (dark gray shaded region), and full range (light gray shaded region) for 10-m wind speed measured at the SIO pier.

shown in Fig. 2*B*, this results in a strong upward flux (sea to air) of $ClNO_2$ that, at its maximum, is approximately half the magnitude of the $N_2O_5$ peak flux. This difference is due to the prescribed $ClNO_2$ product yield coupled to exchange with the bulk ocean. In model case 2 (C2), we set the model input parameters at the 90% confidence limits of those suggested in the literature, in the direction of reducing the upward flux of $ClNO_2$ [e.g., $K_H$ $(ClNO_2)$ = 0.32, $\Phi$ $(ClNO_2)_{ocean}$ = 0.5, $k_r$ = $2 \times 10^5$ $s^{-1}$, $\delta$ = $7.1 \times 10^{-6}$ cm]. This results in a factor of two reduction in peak $ClNO_2$ flux, but the direction of the flux is still positive and outside the uncertainty of the measurements for much of the night. In model case 3 (C3), we take $\Phi$ $(ClNO_2)_{ocean}$ = 0, suggesting that perhaps $NO_2^+$ does not react with $Cl^-$ as expected but proceeds via nitration reactions (36) with enriched organic material found in the sea surface microlayer (23). It is only by setting the $ClNO_2$ product yield to zero or invoking rapid $ClNO_2$ aqueous-phase reaction kinetics or hydrolysis that we can force the model near the uncertainty limits of the measurements.

For the conditions sampled here, $ClNO_2$ production rates were less than $3.0 \times 10^{-3}$ ppt $s^{-1}$ [calculated for the median observed $k_{het}$, $\Phi$ $(ClNO_2)_{ocean}$ = 1, and $[N_2O_5]$ = 50 pptv] and the $ClNO_2$ steady-state lifetime with respect to loss to gas-phase and aerosol reactions is estimated at greater than 30 h (4). As a result, it is unlikely that significant gradients in $ClNO_2$ exist in the nocturnal marine boundary layer due to vertical gradients in the $ClNO_2$ atmospheric production rate. As such, our measurements of the vertical flux of $ClNO_2$, presented here, are most consistent with a model where the product yield of $ClNO_2$ is near zero for reactions of $NO_2^+$ in the sea surface microlayer, and/or $ClNO_2$ aqueous-phase reactions are significantly faster than the volatilization rate.

**Relative Roles of the Particle and Ocean Surface in Regulating $\tau(N_2O_5)$.** To assess the relative roles of the ocean and aerosol surface in the net removal of $N_2O_5$, both reactant transport and surface reactivity must be considered. At a marine boundary layer inversion height ($z_i$) of 810 m, taken as the nocturnally averaged $z_i$ observed during DYCOMS-II off the coast of San Diego (37), the total aerosol surface area ranges between 5% and 50% of the surface area of a slab ocean, based on aerosol surface area measurements made at the SIO pier. In gas–aerosol reactions, transport of the reactant to the particle surface is set by the gas–aerosol collision rate, which is a function of the mean molecular speed of the reactant and the total suspended aerosol surface area (Eq. **E6**). In contrast, reactions occurring at the ocean surface require turbulent transport of the reactants to the diffusive sublayer, where turbulence is suppressed and molecular diffusion controls the collision rate of the reactant with the ocean surface. We compare $N_2O_5$ deposition rates ($k_{dep}$, Eq. **E5**) with $N_2O_5$ heterogeneous aerosol reaction rates ($k_{aerosol}$, Eq. **E6**), both directly measured at the SIO pier.

$$k_{dep} = -\frac{V_{ex}}{z_i} \qquad \textbf{[E5]}$$

$$k_{aerosol} = \frac{\gamma(N_2O_5)\omega S_a}{4} \qquad \textbf{[E6]}$$

Here, $V_{ex}$ is the measured $N_2O_5$ exchange velocity, $z_i$ is the marine boundary layer inversion height, $\gamma(N_2O_5)$ is the $N_2O_5$ reactive uptake coefficient, $\omega$ is the molecular velocity for $N_2O_5$, and $S_a$ is the aerosol surface area concentration. Measurements of $k_{aerosol}$ at this location have been described previously (38), where the median $k_{aerosol}$ was observed to be $6.04 \times 10^{-5}$ $s^{-1}$ with an interquartile range of 4.5–7.4 $\times$ $10^{-5}$ $s^{-1}$, where $k_{aerosol}$ was a strong function of particle nitrate and organic mass fractions. As described above, the mean $V_{ex}$ was $-1.66 \pm 0.60$ cm $s^{-1}$ measured at an average wind speed of 9 m $s^{-1}$, corresponding to a range in $k_{dep}$ of 0.17–1.7 $\times$ $10^{-4}$ $s^{-1}$ for $z_i$ between 1000 and 100 m, respectively.

The relative strengths of the ocean and the aerosol surface in the net removal of $N_2O_5$ from the atmosphere are shown in Fig. 4, where the fraction of $N_2O_5$ lost to the ocean surface is shown as a function of $k_{dep}$ and $k_{aerosol}$. As indicated by the dashed box, the fraction of $N_2O_5$ removed by the ocean surface ranges between 19% and 79% for the conditions sampled at the SIO pier, where shallow boundary layers ($1000 < z_i < 100$ m) and high wind speeds combined with suppressed $N_2O_5$ heterogeneous reactivity, result in large fractions of $N_2O_5$ being lost at the air–sea interface. For $z_i$ = 810 m (37) and $k_{aerosol} = 6.04 \times 10^{-5}$ $s^{-1}$, the fraction of $N_2O_5$ lost at the air–sea interface is 32%, ranging between 26% and 42% for the interquartile range in $k_{aerosol}$. It is important to note that the measurements described here were made at wind speeds significantly larger than the annual median wind speed measured at the SIO pier (2.1 m $s^{-1}$). Based on the parameterized dependence of $K_t$ on wind speed, it is expected that the range in $k_{dep}$ reported in Fig. 4 may be a factor of 3 smaller at lower wind conditions, resulting in the fraction of $N_2O_5$ removed by the ocean surface to between 7% and 55% ($1000 > z_i > 100$ m). In addition, increased aerosol surface area concentrations under low wind speeds, due to reduced dilution of aerosol from an urban source, may also serve to reduce the fraction of $N_2O_5$ removed by the ocean surface at low wind speed.

**$NO_x$ Removal Rates and $ClNO_2$ Production.** At present, the majority of steady-state box model analyses as well as regional-scale chemical transport models designed to assess nocturnal $NO_x$ chemistry do not include either $N_2O_5$ or $ClNO_2$ deposition to the ocean surface or the possibility for reaction at the air–sea interface (39, 40). Here, we use a 0D time-dependent box model to assess the impact of air–sea exchange on $NO_x$ removal rates and Cl atom production rates in the polluted marine boundary layer. The box model was run under four different $N_2O_5$ deposition rates at two different values of $\Phi$ $(ClNO_2)_{ocean}$, 0 and 0.8. It is important to note that the impact of $N_2O_5$ loss mechanisms on $NO_x$ removal rates and Cl atom production is coupled to nitrate radical ($NO_3$) chemistry, where reaction of $NO_3$ with dimethyl sulphide (DMS) can act as the primary loss process for nocturnal nitrogen oxides. In the model described here, DMS concentrations are set to 100 pptv, corresponding to a loss rate of $2.6 \times 10^{-3}$ $s^{-1}$ for $NO_3$. Model details can be found in *SI Text* as well as in *Materials and Methods*.

To assess the importance of deposition processes on reactive nitrogen and halogen budgets in coastal, polluted regions, we

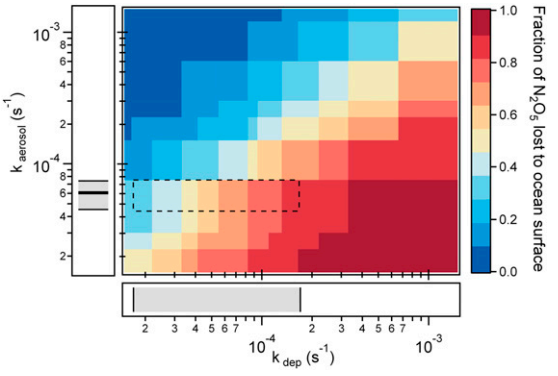


**Fig. 4.** Fraction of the total $N_2O_5$ removal attributed to deposition to the ocean shown as a function of the $N_2O_5$ deposition rate ($k_{dep}$) and the heterogeneous loss rate to aerosols ($k_{aerosol}$). The boxed region represents the range in $k_{dep}$ and $k_{aerosol}$ measured at the SIO pier in La Jolla, CA. The median and interquartile range in the observed $k_{aerosol}$ is shown on the ordinate, while the range in the observed $k_{dep}$ [based on a marine boundary layer inversion height ($z_i$) of 100–1000 m, at an average wind speed of 9.1 $\pm$ 1.3 m $s^{-1}$] is shown on the abscissa.

first examine the fraction of $NO_x$ present at sunset, $[NO_x]_{sunset}$, that is lost to terminal sinks at night as a function of the $N_2O_5$ exchange velocity and $ClNO_2$ product yield.

$$F(NO_x \text{ lost}) = \frac{[NO_x]_{Sunset} - [NO_x]_{Sunrise}}{[NO_x]_{Sunset}} \quad \text{[E7]}$$

As shown in Fig. 5*A*, constraining the model with the measured $V_{ex}$ (−1.66 cm $s^{-1}$), $z_i$ = 500 m and our best estimate of the yield of $ClNO_2$ produced at the ocean surface [$\Phi\ (ClNO_2)_{ocean} = 0$], results in an approximate 14% increase in the fraction of $NO_x$ that is lost to terminal sinks at night, compared with the model that neglects deposition (0.58–0.66). This trend shown in Fig. 5*A* describes the increasing fraction of $NO_x$ that is deposited to the ocean surface, where at the limit of $\Phi\ (ClNO_2)_{ocean} \rightarrow 1$, approximately half of deposited $N_2O_5$ is returned to the atmosphere as $ClNO_2$ and in the limit of $\Phi\ (ClNO_2)_{ocean} \rightarrow 0$, all of the deposited $N_2O_5$ is terminally lost from the atmosphere. Model scenarios that neglect deposition or prescribe a high $ClNO_2$ product yield at the air–sea interface are efficient in recycling $NO_x$, where as much as 50% of reacted $N_2O_5$ is returned as $NO_2$ in the early morning following the photolysis of $ClNO_2$ (Fig. 5*B*). Further, these model scenarios will result in higher concentrations of $ClNO_2$ at sunrise, compared with models that include deposition and low $\Phi\ (ClNO_2)_{ocean}$.

Our observations suggest that $N_2O_5$ deposited to the ocean surface is terminally lost, thus limiting $NO_x$ recycling rates and Cl atom production that would otherwise be sustained by heterogeneous mechanisms at the air–particle interface. As shown in Fig. 5*B*, including deposition to the ocean surface and neglecting $ClNO_2$ surface production results in nearly a 20% reduction in the concentration of $ClNO_2$ at sunrise, compared with a model that does not include $N_2O_5$ deposition. For comparison, including deposition to the ocean surface at the rates measured here, with a high $ClNO_2$ surface yield (0.8), results in nearly a 10% increase in the concentration of $ClNO_2$ at sunrise. This analysis highlights the sensitivity of the nocturnal nitrogen and halogen budget to $N_2O_5$ deposition and the resulting chemistry in the sea surface microlayer.

**Atmospheric Implications.** We present an analysis of direct measurements of $N_2O_5$ and $ClNO_2$ air–sea exchange using eddy covariance. Our results indicate that $N_2O_5$ deposition to the ocean surface is rapid ($V_{ex} = -1.66 \pm 0.60$ cm $s^{-1}$). We find no evidence for net $ClNO_2$ production at the air–sea interface in this study, suggesting either that rates of aqueous-phase reactions of $ClNO_2$ in the sea surface microlayer (SSML) are competitive with volatilization, or that the product yield for $ClNO_2$ is small in the organic-rich SSML. Comparison with direct measurements of the $N_2O_5$ loss rate to aerosol particles at the same sampling location indicates that the ocean surface serves on average to remove 32% of $N_2O_5$ in the marine boundary layer under the conditions sampled here (assuming $z_i$ = 810 m). Our results suggest that future measurements of the exchange velocities of $N_2O_5$ under a wide range of wind conditions will provide needed constraints on parameterizations of the air-side transfer rate ($k_a$). We hypothesize that measurements of the flux of $ClNO_2$ will display large spatiotemporal variability and be responsive to the chemical composition and concentration of dissolved organic material (DOM) in the surface ocean due to the competition reactions of the nitronium ion with DOM and halogen ions. Our results suggest that regional modeling efforts designed to assess the impact of nocturnal nitrogen chemistry on oxidant loadings in coastal polluted environments need to properly represent air–sea interactions for adequate representation of the lifetime of both $N_2O_5$ and $ClNO_2$.

More broadly, we show that direct measurements of trace gas vertical fluxes when combined with in situ determinations of the reactive uptake to aerosol particles provides an experimental constraint on the lifetime and reactivity of trace gases to the wide

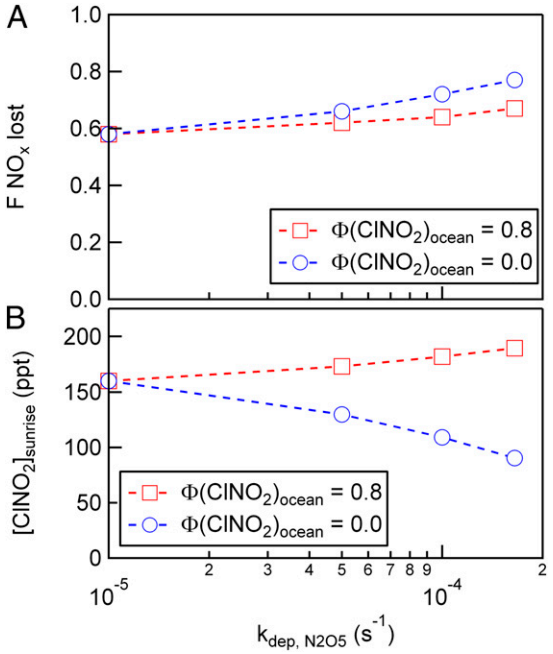


**Fig. 5.** (*A*) Model calculations of the fraction of available $NO_x$ ($[NO_x]_{sunset}$) lost during a 12-h night and (*B*) the mixing ratio of $ClNO_2$ at sunrise as a function of the prescribed $N_2O_5$ exchange velocity and $ClNO_2$ product yield [$\Phi\ (ClNO_2)_{ocean}$]. Calculations were conducted using a 0D time-dependent box model constrained by the mean $N_2O_5$ reactive uptake coefficients and particle surface area (SA) concentrations measured at this site [$\gamma(N_2O_5)$ = 0.005, SA = 500 $\mu m^2$ $cm^3$]. The model was initialized with the following conditions: $T_{air}$ = 283 K, $T_{water}$ = 287 K, $[O_3]_i$ = 60 ppb, $[NO_x]_i$ = 1.0 ppb, $\gamma(NO_3)$ = 0, and $NO_3$ reactivity = 0.16 $min^{-1}$.

array of available surfaces in the marine boundary layer. These results indicate that under conditions of shallow boundary layer heights, uptake to the ocean surface can outpace uptake to aerosol surfaces, highlighting the vast difference in the chemical composition, morphology, phase, and pH of the aerosol and ocean surface. The results presented here highlight the future utility of combining high sensitivity and precision time-of-flight mass spectrometric measurements of reactant and product pairs with micrometeorological techniques for direct, in situ study of chemical reactions occurring at the air–sea interface. This approach will permit study of complex interfacial processes under ambient conditions, where coupled biological, chemical, and physical mechanisms often prohibit the extension of laboratory results to environmental conditions.

## Materials and Methods

**Sampling Location.** Concentration and vertical flux measurements of $N_2O_5$ and $ClNO_2$ were made at 10 m from the northwest boom of the 330-m SIO Pier during February 2013. Air sampled at this location is impacted by local emissions in the La Jolla cove region as well as regional pollution attributed to both San Diego and Los Angeles. The observations presented here are for time periods where winds were sustained from the west (true wind direction between 205° and 295°) so as to ensure an ocean fetch. Backward air trajectories indicate that air sampled during these time periods was influenced by the Los Angeles plume, thus sustaining concentrations of $N_2O_5$ well above that observed in clean, marine air (41).

**$N_2O_5$ and $ClNO_2$ Concentration Measurements.** $N_2O_5$ and $ClNO_2$ mixing ratios were measured using chemical ionization time-of-flight mass spectrometry (24), using $I^-$ reagent ion chemistry (25). $N_2O_5$ sensitivities were determined using the output of a portable $N_2O_5$ generation system, described previously (42), where $N_2O_5$ is made in situ from the dark reaction of $NO_2$ and $O_3$, and subsequent reaction of the $NO_3$ product with $NO_2$. $ClNO_2$ sensitivities were determined by passing the output of the $N_2O_5$ source over concentrated NaCl slurry for unit conversion of $N_2O_5$ to $ClNO_2$ (4, 25, 43). We sample $N_2O_5$

and $ClNO_2$ through a 17-m, 3/8" o.d. Teflon perfluoroalkoxy tube. The inlet manifold is constructed of fluoropel-coated glass, closely resembling that of Ellis et al. (44), where air is drawn through a critical orifice, reducing the sample line pressure to 200 mbar. The resulting mass flow rate of 10 standard liters per minute results in a laminar flow profile, with a measured gas exchange time for the inlet of 0.7 s.

**$N_2O_5$ and $ClNO_2$ Flux Measurements.** Mass spectra, acquired at 80 kHz, were saved at 10 Hz, coincident with measurements of 3D winds acquired with a colocated ultrasonic anemometer sampling at 20 Hz (HS-50; Gill Instruments). Fluxes were determined by the eddy covariance technique (45). In this method, the vertical turbulent flux is the covariance of vertical wind speed ($w$) and mixing ratio from the mean ($c$), $F = \langle w'c' \rangle$. Details on the application of time of flight mass spectrometry to eddy covariance flux measurement can be found elsewhere (46) and described in more detail in *SI Text*.

**Time-Dependent Air–Sea Model.** The chemical evolution of the nocturnal boundary layer was tracked using a one-dimensional time-dependent dimensional box model, where coupled differential equations were solved using custom code written in MATLAB, analyzed with the built-in ordinary differential equation solvers. As time propagates in the model, we calculate the production and loss of NO, $NO_2$, $O_3$, $N_2O_5$, $NO_3$, $HNO_3$, and $ClNO_2$ to gas-phase and heterogeneous reactions occurring on/within aerosol particles, as well as air–sea exchange with the ocean surface. The model is initialized with concentrations representative of those measured at the SIO pier, and reaction rates from the NASA Jet Propulsion Laboratory Chemical Kinetics and Photochemical Data for Use in Atmospheric Studies, Evaluation Number 14. Detailed descriptions of the modeling efforts described here can be found in *SI Text*.

**ACKNOWLEDGMENTS.** We thank Byron Blomquist (University of Hawaii) and Joel Thornton (University of Washington) for helpful discussions and Christian McDonald (SIO), Nicole Campbell [University of California, San Diego (UCSD)], and Kathryn Zimmerman (UCSD) for assistance in the setup for the pier observations. This research was supported by the National Science Foundation CAREER Award to T.H.B. (Grant AGS-1151430).

1. Alexander B, et al. (2009) Quantifying atmospheric nitrate formation pathways based on a global model of the oxygen isotopic composition ($\Delta^{17}O$) of atmospheric nitrate. *Atmos Chem Phys* 9(14):5043–5056.
2. Behnke W, George C, Scheer V, Zetzsch C (1997) Production and decay of $ClNO_2$, from the reaction of gaseous $N_2O_5$ with NaCl solution: Bulk and aerosol experiments. *J Geophys Res-Atmos* 102(D3):3795–3804.
3. Finlayson-Pitts BJ, Ezell MJ, Pitts JN (1989) Formation of chemically active chlorine compounds by reactions of atmospheric NaCl particles with gaseous $N_2O_5$ and $ClONO_2$. *Nature* 337(6204):241–244.
4. Osthoff HD, et al. (2008) High levels of nitryl chloride in the polluted subtropical marine boundary layer. *Nat Geosci* 1(5):324–328.
5. Thornton JA, et al. (2010) A large atomic chlorine source inferred from mid-continental reactive nitrogen chemistry. *Nature* 464(7286):271–274.
6. Aldener M, et al. (2006) Reactivity and loss mechanisms of $NO_3$ and $N_2O_5$ in a polluted marine environment: Results from in situ measurements during New England Air Quality Study 2002. *J Geophys Res*, 10.1029/2006JD007252.
7. Huff DM, Joyce PL, Fochesatto GJ, Simpson WR (2011) Deposition of dinitrogen pentoxide, $N_2O_5$, to the snowpack at high latitudes. *Atmos Chem Phys* 11(10): 4929–4938.
8. Hinrichsen D (1998) *Coastal Waters of the World: Trends, Threats, and Strategies* (Island Press, Washington, DC).
9. Wagner NL, et al. (2012) The sea breeze/land breeze circulation in Los Angeles and its influence on nitryl chloride production in this region. *J Geophys Res*, 10.1029/2012JD017810.
10. Liss PS, Slater PG (1974) Flux of gases across air-sea interface. *Nature* 247(5438): 181–184.
11. Carpenter LJ, Archer SD, Beale R (2012) Ocean-atmosphere trace gas exchange. *Chem Soc Rev* 41(19):6473–6506.
12. Thornton JA, Braban CF, Abbatt JPD (2003) $N_2O_5$ hydrolysis on sub-micron organic aerosols: The effect of relative humidity, particle phase, and particle size. *Phys Chem Chem Phys* 5(20):4593–4603.
13. Bertram TH, Thornton JA (2009) Toward a general parameterization of $N_2O_5$ reactivity on aqueous particles: The competing effects of particle liquid water, nitrate and chloride. *Atmos Chem Phys* 9(21):8351–8363.
14. Mentel TF, Sohn M, Wahner A (1999) Nitrate effect in the heterogeneous hydrolysis of dinitrogen pentoxide on aqueous aerosols. *Phys Chem Chem Phys* 1(24):5451–5457.
15. Wahner A, Mentel TF, Sohn M, Stier J (1998) Heterogeneous reaction of $N_2O_5$ on sodium nitrate aerosol. *J Geophys Res* 103(D23):31103–31112.
16. Anttila T, Kiendler-Scharr A, Tillmann R, Mentel TF (2006) On the reactive uptake of gaseous compounds by organic-coated aqueous aerosols: Theoretical analysis and application to the heterogeneous hydrolysis of $N_2O_5$. *J Phys Chem A* 110(35):10435–10443.
17. Cosman LM, Bertram AK (2008) Reactive uptake of $N_2O_5$ on aqueous $H_2SO_4$ solutions coated with 1-component and 2-component monolayers. *J Phys Chem A* 112(20): 4625–4635.
18. McNeill VF, Patterson J, Wolfe GM, Thornton JA (2006) The effect of varying levels of surfactant on the reactive uptake of $N_2O_5$ to aqueous aerosol. *Atmos Chem Phys* 6(6): 1635–1644.
19. Escorcia EN, Sjostedt SJ, Abbatt JPD (2010) Kinetics of N(2)O(5) hydrolysis on secondary organic aerosol and mixed ammonium bisulfate-secondary organic aerosol particles. *J Phys Chem A* 114(50):13113–13121.
20. Roberts JM, et al. (2009) Laboratory studies of products of $N_2O_5$ uptake on $Cl^-$ containing substrates. *Geophys Res Lett*, 10.1029/2009GL040448.
21. Griffiths PT, et al. (2009) Reactive uptake of N2O5 by aerosols containing dicarboxylic acids. Effect of particle phase, composition, and nitrate content. *J Phys Chem A* 113(17):5082–5090.
22. Fried A, Henry BE, Calvert JG, Mozurkewich M (1994) The reaction probability of $N_2O_5$ with sulfuric acid aerosols at stratospheric temperatures and compositions. *J Geophys Res* 99(D2):3517–3532.
23. Hunter KA, Liss PS (1977) Input of organic material to oceans: Air-sea interactions and organic chemical composition of sea surface. *Mar Chem* 5(4-6):361–379.
24. Bertram TH, et al. (2011) A field-deployable, chemical ionization time-of-flight mass spectrometer. *Atmos Meas Tech* 4(7):1471–1479.
25. Kercher JP, Riedel TP, Thornton JA (2009) Chlorine activation by $N_2O_5$: Simultaneous, in situ detection of $ClNO_2$ and $N_2O_5$ by chemical ionization mass spectrometry. *Atmos Meas Tech* 2(1):193–204.
26. Nelson HH, Johnston HS (1981) Kinetics of the reaction of Cl with ClNO and $ClNO_2$ and the photochemistry of $ClNO_2$. *J Phys Chem* 85(25):3891–3896.
27. Riedel TP, et al. (2012) Nitryl chloride and molecular chlorine in the coastal marine boundary layer. *Environ Sci Technol* 46(19):10463–10470.
28. Fairall CW, Helmig D, Ganzeveld L, Hare J (2007) Water-side turbulence enhancement of ozone deposition to the ocean. *Atmos Chem Phys* 7(2):443–451.
29. Johnson MT (2010) A numerical scheme to calculate temperature and salinity dependent air-water transfer velocities for any gas. *Ocean Sci* 6(4):913–932.
30. Mackay D, Yeun ATK (1983) Mass transfer coefficient correlations for volatilization of organic solutes from water. *Environ Sci Technol* 17(4):211–217.
31. Fairall CW, Bradley EF, Hare JE, Grachev AA, Edson JB (2003) Bulk parameterization of air-sea fluxes: Updates and verification for the COARE algorithm. *J Clim* 16(4): 571–591.
32. Robinson GN, Worsnop DR, Jayne JT, Kolb CE, Davidovits P (1997) Heterogeneous uptake of $ClONO_2$ and $N_2O_5$ by sulfuric acid solutions. *J Geophys Res* 102(D3): 3583–3601.
33. Liss PS (1973) Processes of gas exchange across an air-water interface. *Deep Sea Res* 20(3):221–238.
34. Duce RA, et al. (1991) The atmospheric input of trace species to the world ocean. *Global Biogeochem Cycles* 5(3):193–259.
35. Carpenter LJ, et al. (2013) Atmospheric iodine levels influenced by sea surface emissions of inorganic iodine. *Nat Geosci* 6(2):108–111.
36. Heal MR, Harrison MAJ, Cape JN (2007) Aqueous-phase nitration of phenol by $N_2O_5$ and $ClNO_2$. *Atmos Environ* 41(17):3515–3520.
37. Faloona I, et al. (2005) Observations of entrainment in eastern Pacific marine stratocumulus using three conserved scalars. *J Atmos Sci* 62(9):3268–3285.
38. Riedel TP, et al. (2012) Direct $N_2O_5$ reactivity measurements at a polluted coastal site. *Atmos Chem Phys* 12(6):2959–2968.
39. Brown SS, Stutz J (2012) Nighttime radical observations and chemistry. *Chem Soc Rev* 41(19):6405–6447.
40. Saiz-Lopez A, von Glasow R (2012) Reactive halogen chemistry in the troposphere. *Chem Soc Rev* 41(19):6448–6472.
41. Draxler RR, Rolph GD (2013) HYSPLIT (HYbrid Single-Particle Lagrangian Integrated Trajectory) Model access via NOAA ARL READY Web site (www.arl.noaa.gov/ready/hysplit4.html), NOAA Air Resources Laboratory. Silver Spring, MD.
42. Bertram TH, Thornton JA, Riedel TP (2009) An experimental technique for the direct measurement of $N_2O_5$ reactivity on ambient particles. *Atmos Meas Tech* 2(1):231–242.
43. Thaler RD, Mielke LH, Osthoff HD (2011) Quantification of nitryl chloride at part per trillion mixing ratios by thermal dissociation cavity ring-down spectroscopy. *Anal Chem* 83(7):2761–2766.
44. Ellis RA, et al. (2010) Characterizing a Quantum Cascade Tunable Infrared Laser Differential Absorption Spectrometer (QC-TILDAS) for measurements of atmospheric ammonia. *Atmos Meas Tech* 3(2):397–406.
45. Baldocchi DD, Hicks BB, Meyers TP (1988) Measuring biosphere-atmosphere exchanges of biologically related gases with micrometeorological methods. *Ecology* 69(5):1331–1340.
46. Farmer DK, et al. (2011) Eddy covariance measurements with high-resolution time-of-flight aerosol mass spectrometry: A new approach to chemically resolved aerosol fluxes. *Atmos Meas Tech* 4(6):1275–1289.